Journal of Materials Science and Emerging Technologies

SCIVOLVE

Research Article

Open Access Full Text Article

Antibacterial Investigation of Cu and CuO Based PSF/PVP Composite Membranes

William M. Motswainyana[1]*, Bakang F. Modukanele[1], Adewale O. Adeloye[1,2]

[1]*Botswana Institute for Technology Research and Innovation, Maranyane House, Plot 50654 Machel Drive, Gaborone, Botswana.*
[2]*Department of Analytical, Colloid Chemistry and Technology of Rare Elements, al-Farabi Kazakh National University, Almaty. Republic of Kazakhstan, 050040.*

***Correspondence:**

William M. Motswainyana
Botswana Institute for Technology Research and Innovation, Maranyane House, Plot 50654 Machel Drive, Gaborone, Botswana.

Received: April 02, 2026; **Published:** April 24, 2026.

How to cite this article:

W. M. Motswainyana, B. F. Modukanele, and A. O. Adeloye, "Antibacterial investigation of Cu and CuO based PSF/PVP composite membranes," *Journal of Materials Science and Emerging Technologies*, vol. 1, no. 1, pp. 1–8, 2026.

Abstract

In this work, we report fabrication and antimicrobial activity of PSF/PVP based Cu and CuO membranes against human gram-negative bacteria Escherichia coli. These membranes were fabricated by electrospinning and have been fully characterized, including SEM, EDX and X-ray diffraction. SEM images of the composite membranes clearly showed presence and distribution of Cu and CuO nanoparticles on the PSF/PVP fiber surfaces. The PSF/PVP based Cu and CuO nanoparticles membranes exhibited significant antibacterial activity against E. coli, with no evidence of leaching, thereby positioning the composite membranes as potential antibacterial materials for water filtration, protective clothing and wound healing.

Keywords: Nanoparticles; electrospinning; fibers; membranes; antimicrobial

1. Introduction

There is growing research interest in developing alternative antimicrobial agents triggered by the spread of antibiotic-resistant infections [1]. These alternative materials include antibiotics, cationic polymers, antimicrobial peptides and metal nanoparticles [2]. Metal nanoparticles are mostly utilized in antibacterial coatings as implantable devices and medicinal materials for various purposes: to prevent infection and promote wound healing, to treat diseases in antibiotic delivery systems; to generate microbial diagnostics in bacterial detection systems; and to control bacterial infections in antibacterial vaccines [3,4]. Their preference as an alternative to antibiotics is premised on existing evidence that nanoparticles effectively prevent microbial drug resistance in certain cases [3,4,5].

However, antibacterial mechanisms of these nanoparticles are poorly understood, but the accepted mechanisms include oxidative stress induction, metal ion release and non-oxidative mechanisms [3]. Cu nanoparticles have exhibited antibacterial effect on the bacterial cell functions in multiple ways, including adhesion to Gram negative bacterial cell walls [6]. Their efficacy is not surprising because Cu nanoparticles have larger specific surface area compared to their copper metal counterpart, which allows them to interact closely with microbial membranes [6]. Similarly, CuO nanoparticles have great biological properties including effective antimicrobial action against a wide range of pathogens and drug resistant bacteria, although they have not yet been investigated as efficient drug delivery system [7,8]. These properties have led to the development of various approaches with direct applications of nanoparticles to the biomedical field, such as tailored surfaces with antimicrobial effect, wound dressings and modified textiles [9]. There are future prospects for biomedical applications of CuO nanoparticles in areas such as detection of viruses in the human body [8].

Incorporation of metal nanoparticles on polymer nanofibers and other composites has paved way to enhancing their microbial behavior [10,11]. The nanoparticle-incorporated biomaterials provide perfect composite material with improved properties and activated therapeutics [12]. The structural properties of these composite biomaterials, and the arrangement of each constituent of nanoparticles synergistically enhance biomedical capabilities [12]. Consequently, fabrication of polymer composites has emerged as an effective way of expanding the applications of biocidal metals, and the incorporation of metal nanoparticles into

a polymer composite regulates the possibility of loss of particles or ions [11,12]. However, there are drawbacks associated with incorporation of nanoparticles into polymeric membranes. For example, the dispersion behavior control is very difficult for nanoparticles with less than 100 nm due to surface interactions [12,13].

The most used approach to incorporate nanoparticles on nanofibers is electrospinning. This is an established technique of scaffold fabrication offering a number of key advantages which include its facile nature, with electrospun materials offering a high surface area to volume ratio, potential for the release of drugs and antimicrobials, controllable fiber diameters and high porosity and permeability [14]. The electrospinning technique provides non-woven fibers to the order of few nanometers with large surface areas, superior mechanical properties and ease of functionalization for various purposes [15]. Several application areas utilize the technique of electrospinning, and these include biomedical field, filtration and protective material, sensors, electrical and optical applications [15]. In the context of this background, we report fabrication and antimicrobial activity of Polysulfone/ Polyvinylpyrrolidone based Cu and CuO nanoparticles composite membranes against human gram-negative bacteria Escherichia coli. The membranes were fabricated by electrospinning and have been fully characterized. Polysulfone (PSf) is a favorite polymer for the production of membranes due to its excellent physicochemical properties, which include thermal stability; good chemical resistance to different materials such as different bases, acids and chlorine; sufficient mechanical strength; and good processability [16,17]. The polymer is commonly used in applications such as water and wastewater treatment, membrane distillation, blood purification, pollutant removal, gas separation, and support of composite membranes [17]. However, polysulfone membranes have low antifouling performance and low membrane flux values due to their low hydrophilic nature [18]. Addition of hydrophilic polymers such as polyvinyl pyrrolidone (PVP) to the spinning solution is often performed to increase membrane permeability and antifouling ability [18,19].

2. Experimental Section

2.1 Materials

Copper (II) sulphate pentahydrate ($CuSO_4.5H_2O$), copper (II) chloride dihydrate ($CuCl_2.2H_2O$), sodium borohydride ($NaBH_4$), sodium hypophosphite (NaH_2PO_2), sodium hydroxide (NaOH), ethanol (EtOH, 99.8%), ethylene glycol, N,N-dimethylacetamide (DMAc, 99.9%) and the polymers polysulfone, PSF (M_w = 35000) and polyvinylpyrrolidone, PVP (M_w = 360000) were purchased from Sigma-Aldrich and were used as received.

2.2 Fabrication of composite membranes

Cu and CuO nanoparticles were prepared following literature reports [20,21]. Electrospinning experiments were carried out on a FLUIDNATEK LE-100 electrospinning unit. In a typical preparation of spinning solution, PSF/PVP based nanoparticle solution was prepared by dispersing nanoparticles in DMAc via sonication, followed by addition of PSF and PVP into the nanoparticle suspension. A homogeneous solution was attained after 12 h of stirring at room temperature. Fiber formation was achieved by electrospinning the solutions under high voltage. The suitable voltage required to create a Taylor cone was within the range 25-30 kV, and the applied voltage transformed the polymer solution into a charged jet stream. The polymer jet streams were deposited on a rotating or stationery collector. Furthermore, the suitable feed was established to be in the range 1.0-2.8 mL/hr, while the sufficient flight distance for the polymer jet fell within the range 15-25 cm.

2.3 Characterization of composite membranes

Characterization and morphological analysis of the nanoparticles and their respective PSF/PVP based nanoparticle fibers were performed using SHIMADZU IRTracer-100 Fourier Transform Infrared Spectrophotometer, SHIMADZU UV-2600 UV-VIS Spectrophotometer, Empyrean Pananalytical X-ray diffractometer and GeminiSEM 500 Scanning Electron Microscope.

2.4 Antimicrobial assay

Antibacterial activities of PSF/PVP/Cu and PSF/PVP/CuO nanofiber scaffolds were measured by disc diffusion method [22]. *E.coli* was cultured in Müller-Hinton broth for 20 h at 37°C before the test. 100 µL of standardized suspensions for the bacteria was placed on Müller-Hinton agar plates according to McFarland scale (1.3×10^6 CFU/mL). Disc shape samples of PSF/PVP/Cu and PSF/PVP/CuO nanofiber scaffolds of diameter 12 mm were prepared and subjected to the inhibition zone tests. The discs were sterilized with ultraviolet light for 2 hours and subsequently placed on *E. coli* culture plates. The agar plates were incubated for 24 hours at 37°C. The relative antibacterial effect was found by measuring the clear zones of inhibition formed around the discs.

3. Results and Discussion

3.1 Synthesis of Cu and CuO nanoparticles

PVP capped Cu and CuO nanoparticles were prepared by chemical reduction following literature reports [20,21] and the nanoparticles were obtained in powder form in their respective reddish brown and dull brown colors (Fig. 1). These nanoparticles were fully characterized to confirm their successful formation.

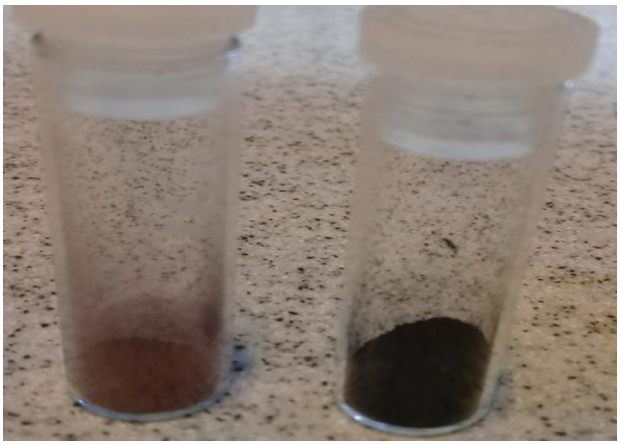

Fig. 1 Camera image of PVP capped Cu and CuO nano-powders

3.2 Characterization of Cu and CuO nanoparticles

3.2.1 UV-vis spectroscopic analysis

UV-vis analysis of the nanoparticles yielded characteristic SPR band of Cu and CuO nanoparticles at around 580 nm and 360 nm respectively (Fig. 2). The UV-vis results agreed with previous literature reports [23,24]. The peak sharpness remained unchanged after 3 weeks of storage in ethanol, thereby suggesting that the nanoparticles were stable over long periods, owing to the PVP capping.

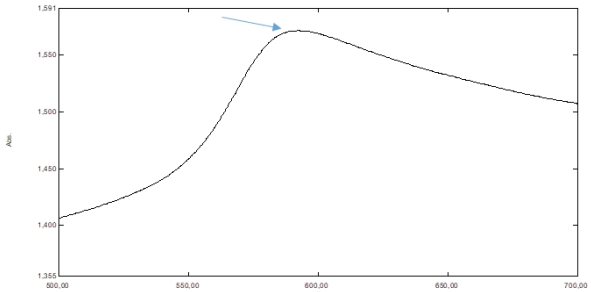

Fig. 2A UV-vis spectrum of PVP capped Cu nanoparticles

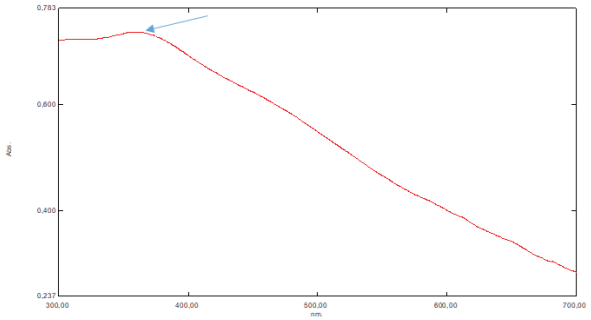

Fig. 2B UV-vis spectrum of PVP capped CuO nanoparticles

3.2.2 SEM and EDAX analysis

In the SEM analysis of the nanoparticles, Cu nanoparticles appeared as a mixture of cubic and spherically shaped particles, with evidence of agglomeration (Fig. 3A). Furthermore, EDAX analysis of Cu nanoparticles showed signals for elemental Cu as expected (Fig. 3B). Similarly, SEM image of CuO nanoparticles showed several kinds of CuO particles with different morphologies, which included spherical-shaped, sheet-shaped and rod-shaped (Fig. 4A). The elemental composition of CuO nanoparticles studies by EDAX, showed strong peaks which confirmed the presence of copper and oxygen (Fig. 4B). The SEM data was supported by already existing literature reports [20,25,26].

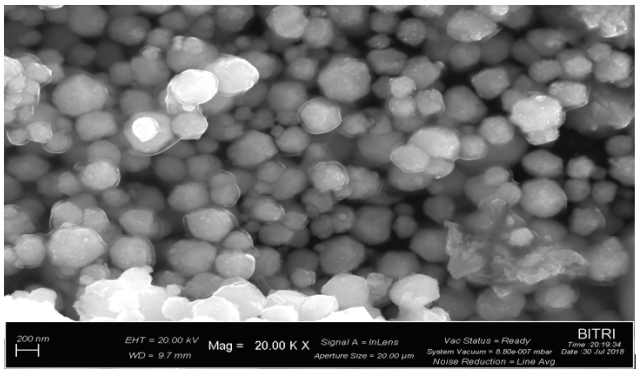

Fig. 3A SEM image of PVP capped Cu nanoparticles

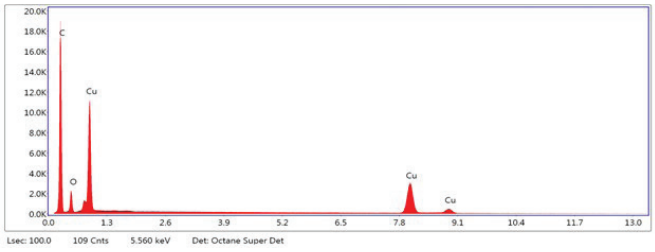

Fig. 3B EDX spectrum of PVP capped Cu nanoparticles

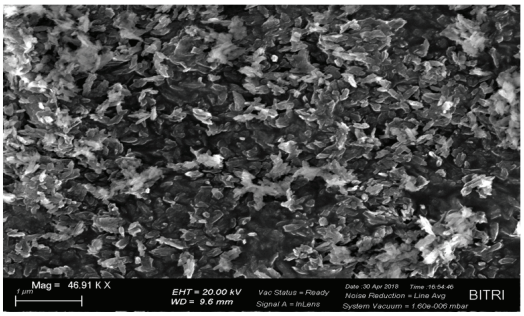

Fig. 4A SEM image of PVP capped CuO nanoparticles

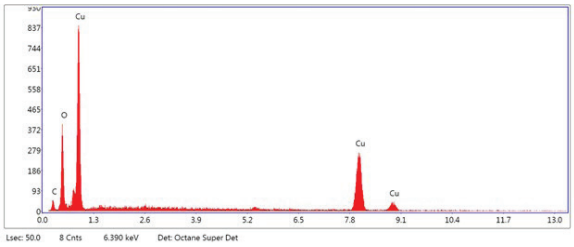

Fig. 4B EDX spectrum of PVP capped CuO nanoparticles

3.2.3 X-ray diffraction analysis

XRD pattern of Cu nanoparticles revealed a mixture of metallic Cu and Cu_2O, with percentage purities of 95.7% and 4.7% respectively (Fig. 5A). This is an illustration that the zero-valent copper nanoparticles formed in the chemical reduction stage go through decomposition due to limited stability of Cu [27]. Therefore, the detected Cu_2O may have been formed by partial oxidation of Cu nanoparticles [28,29]. The diffraction data showed the formation of pure crystalline metallic phase Cu NPs with face centered cubic (FCC) structures with characteristic peaks indexed to (111), (020) and (022) at corresponding 2θ values 43.49º, 50.62º and 74.28º respectively [29]. The diffraction pattern of CuO nanoparticles (Fig. 5B) was characterized by two main diffraction peaks at 2θ values 35.79° and 38.83°, whose position and relative intensity agree perfectly with literature report [30] and ICSD File No. 43180, corresponding to the crystal system of monoclinic CuO space group.

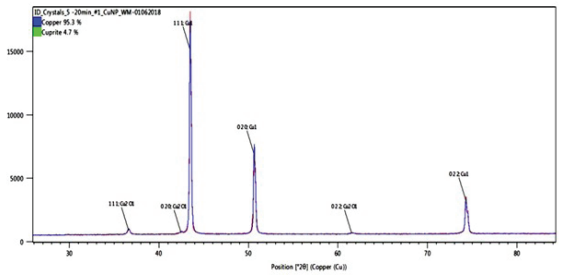

Fig. 5A X-ray diffraction pattern of Cu nanoparticles

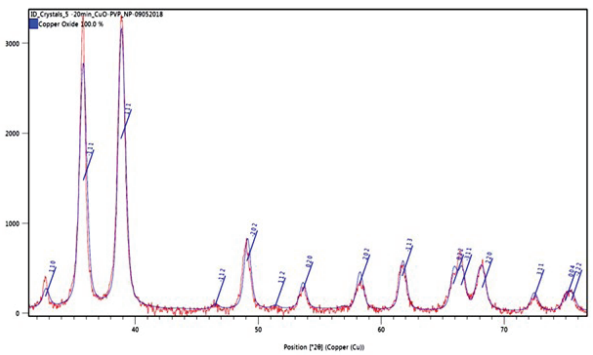

Fig. 5B X-ray diffraction pattern of CuO nanoparticles

3.3 Fabrication of PSF/PVP/Cu and PSF/PVP/CuO composite membranes

PSF/PVP/Cu and PSF/PVP/CuO composite membranes were fabricated via electrospinning of blend solutions of PSF, PVP and the respective nanoparticles in DMAc. The preparation started with dispersion Cu and CuO nanoparticles in DMAc before adding PSF and PVP to obtain a spinning blend solution (Fig. 6A). The composite membranes were obtained in their respective colors of the nanoparticle blend solutions (Fig. 6B).

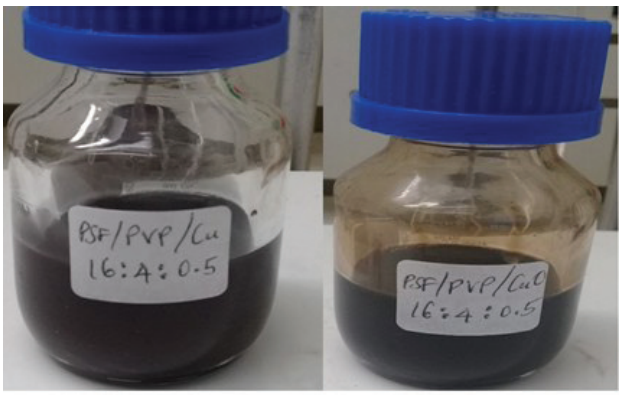

Fig. 6A Camera images of PSF/PVP/Cu and PSF/PVP/CuO blend solutions

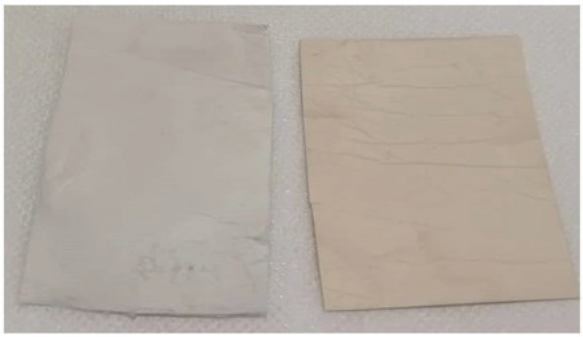

Fig. 6B Camera images of PSF/PVP/Cu and PSF/PVP/CuO composite membranes

3.4 Characterization of PSF/PVP/Cu and PSF/PVP/CuO composite membranes

3.4.1 FTIR analysis

Blending of PSF with PVP was justified by FTIR analysis of the membranes to identify the vibration frequency peaks of PSF and PVP before and after blending. FT-IR spectra of PSF, PVP and PSF/PVP (16:4) blend are presented in Fig. 7A. Absorption bands due to ring stretching vibrations in PSF were observed at 1586, 1490, 1318 and 1243 cm^{-1}, which was ascribed to the ν(C = C), ν(C – H), ν(CH_3), and ν(C – O) respectively [18]. The other observed bands at 1151 and 1013 cm^{-1} were attributed to ν(S = O) and ν(C – O) for the sulphone and ethereal groups in PSF. The IR spectrum of free PVP showed absorption bands at 1692, 1558, 1507, 1419 and 1287 cm^{-1}. These bands were assigned to the ν(C = O), ν(C = C), ν(C – N), ν(C – H), and ν(CH_2) vibrations respectively [18]. For the PSF/PVP polymer blend, three prominent features were observed in the spectrum: a shift to lower vibration frequency from 1692 to 1683 cm^{-1} in the C=O band, complete loss of vibration frequency peak at 1287 cm^{-1} (–CH2–) in PVP, and concomitant decrease in intensity of these signals [18]. For the PSF/PVP blend containing nanoparticles, FTIR spectral patterns generally showed loss of vibration frequency in the C=O band (Fig. 7B), thereby confirming the presence of nanoparticles in the PSF/PVP blend.

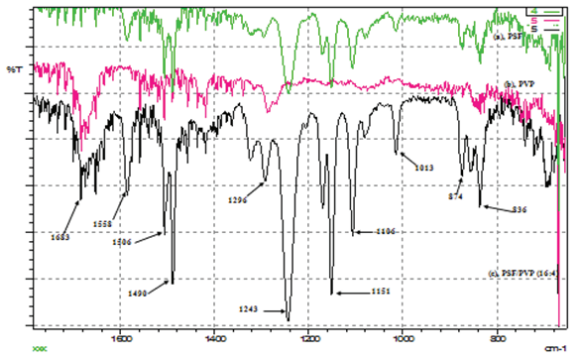

Fig. 7A FTIR of spectra of PSF, PVP and PSF/PVP blend

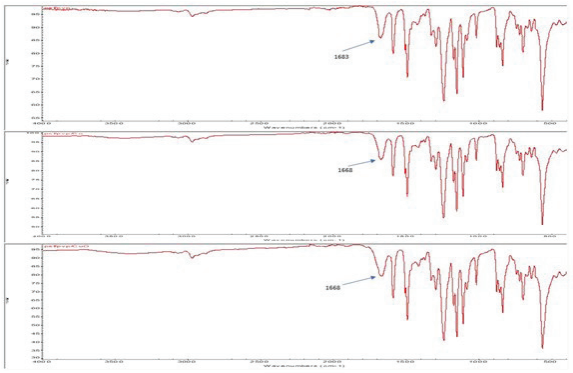

Fig. 7B FTIR spectra of PSF/PVP/Cu and PSF/PVP/CuO composite membranes

3.4.2 UV-vis spectroscopic analysis

UV-vis reflectance spectroscopy of PSF/PVP/Cu and PSF/PVP/CuO membranes showed SPR peaks at 580 nm and 355 nm (Fig. 8) which fell within characteristic surface plasmon resonance ranges of Cu and CuO nanoparticles respectively [23,24]. These peaks confirmed the presence of Cu and CuO nanoparticles in the PSF/PVP blend.

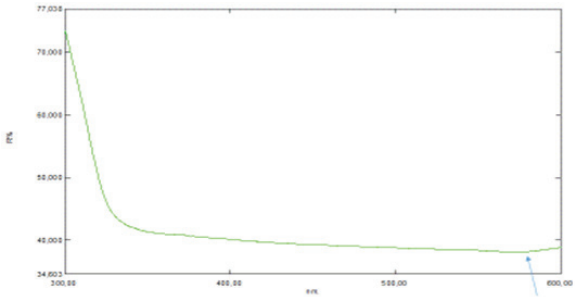

Fig. 8A UV-vis reflectance spectrum of PSF/PVP/Cu membrane

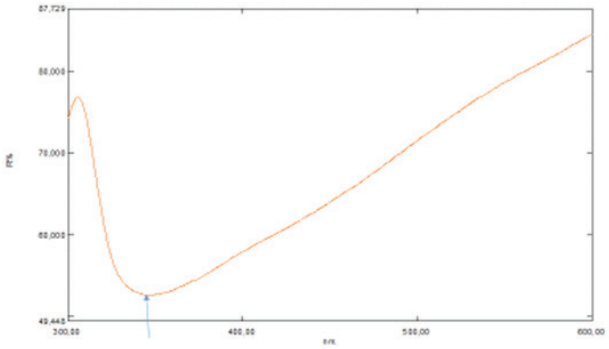

Fig. 8B UV-vis reflectance spectrum of PSF/PVP/CuO membrane

3.4.3 X-ray diffraction analysis

Interaction between PSF/PVP polymer blend and the respective nanoparticles was confirmed by XRD. XRD spectrum of PSF/PVP (Fig. 9A) exhibits one broad diffraction peak at 2θ value of 17.75°, which agrees well with literature [20]. This peak was well maintained after encapsulation of the nanoparticles inside the PSF/PVP matrix. The diffraction pattern for PSF/PVP/Cu (Fig. 9B) showed the presence of pure crystalline metallic phase Cu NPs with face centered cubic (FCC) structures with characteristic peaks indexed to (111), (020), (022) and (131) at corresponding 2θ values 43.34º, 50.48º, 74.18º and 90.01º respectively [29]. There was no evidence of peaks due to cuprous oxide (Cu_2O). Furthermore, the diffraction pattern of PSF/PVP/CuO (Fig. 9C) was characterized by diffraction peaks at 2θ values 35.54° and 38.95°, whose position and relative intensity agreed perfectly with literature report [30] and ICSD File No. 43180.

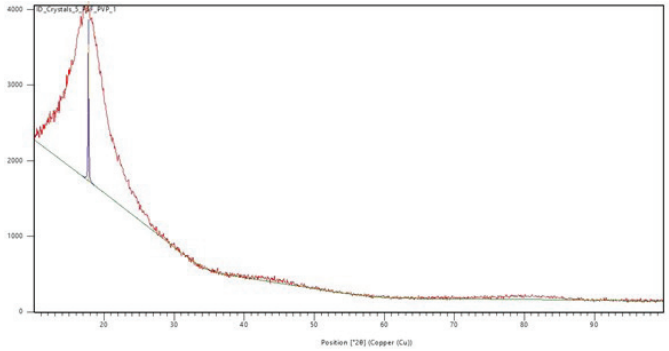

Fig. 9A X-ray diffraction pattern of PSF/PVP membrane

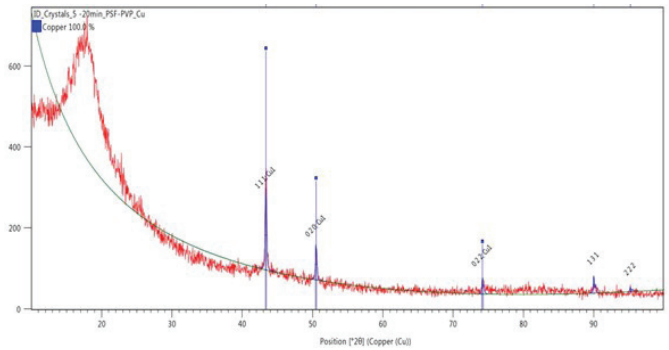

Fig. 9B X-ray diffraction pattern of PSF/PVP/Cu membrane

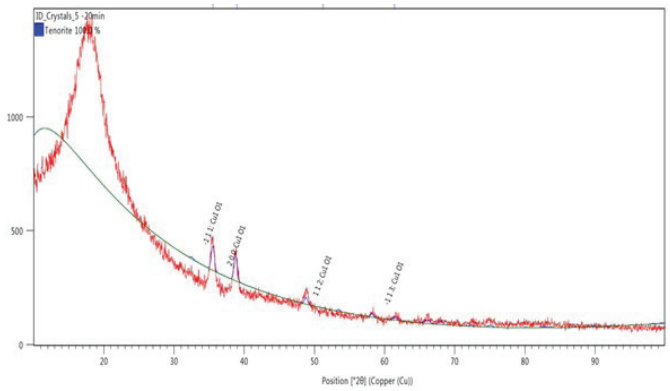

Fig. 9C X-ray diffraction pattern of PSF/PVP/CuO membrane

3.4.4 SEM and EDAX analysis

The morphologies of PSF/PVP/Cu and PSF/PVP/CuO membranes showed continuous fibers of differing sizes with visible white spots on their surfaces, thereby confirming presence of Cu (Fig. 10) and CuO nanoparticles (Fig. 11) within the fibers. The spots are well distributed within the fibers. Further confirmation for the presence of elemental Cu and O in the PSF/PVP membrane was carried out by Energy-dispersive spectroscopy (EDAX), which revealed strong signals of the respective nanoparticles. elemental Cu signals showed up at around 0.8 keV, 8.0 KeV and 9.0 keV (Fig. 10B and 11B).

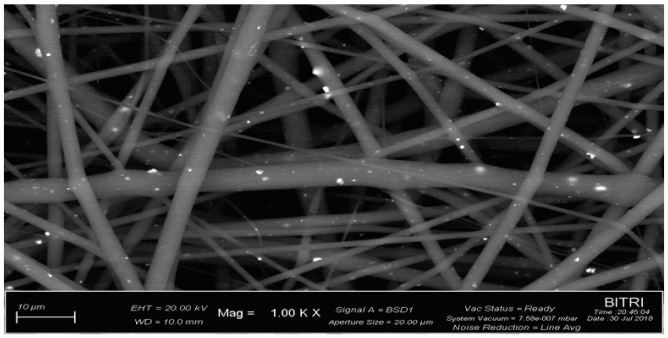

Fig. 10A SEM image of PSF/PVP/Cu membrane

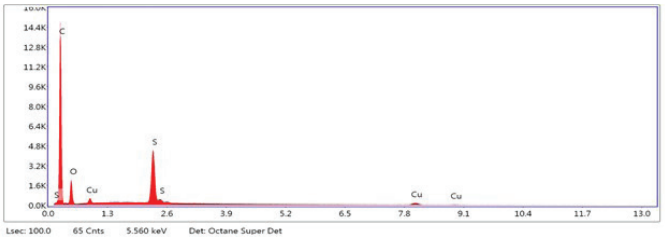

Fig. 10B EDAX analysis of PSF/PVP/Cu membrane

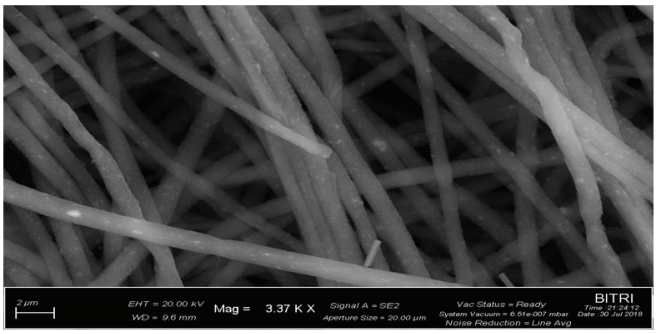

Fig. 11A SEM image of PSF/PVP/CuO membrane

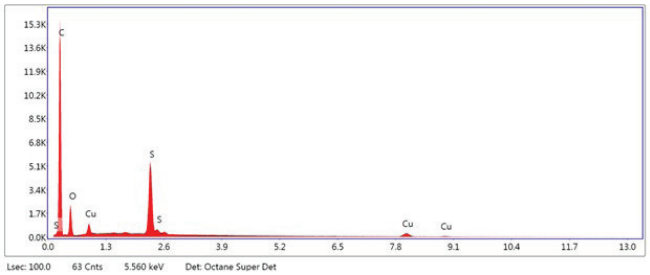

Fig. 11B EDAX analysis of PSF/PVP/CuO membrane

3.5 Antimicrobial investigation

3.5.1 Leaching experiments

Leaching experiments were carried out to determine the likelihood of Cu and CuO to leach out of the blend. PSF/PVP/Cu and PSF/PVP/CuO membranes were soaked in water for 10 days, after which the resultant solution was analyzed for possible leaching of

nanoparticles. However, upon observation after 10 days, there was no visible color change in the soaked PSF/PVP/Cu and PSF/PVP/CuO membranes. UV-vis analysis of the water showed that there was no presence of Cu or CuO nanoparticles in water (Fig. 12).

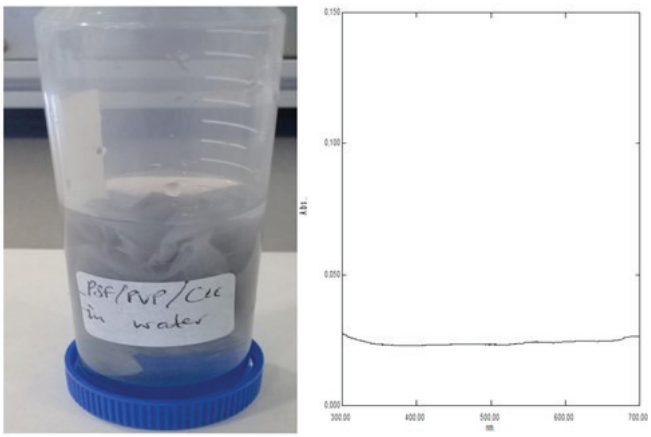

Fig. 12A Soaked PSF/PVP/Cu membrane in water and UV-vis spectrum of water solution following 10 days of soaking

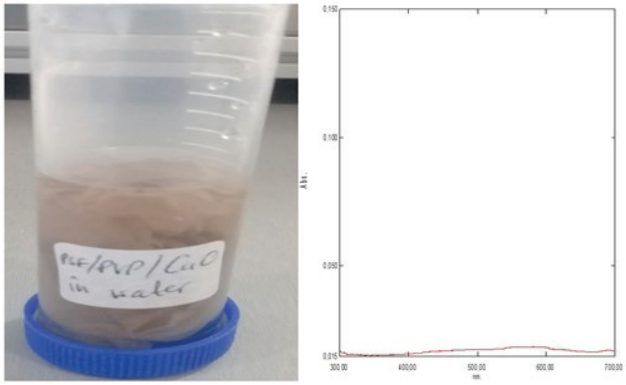

Fig. 12B Soaked PSF/PVP/CuO membrane in water and UV-vis spectrum of water solution following 10 days of soaking

3.5.2 Antimicrobial efficacy

Antimicrobial activity of Cu nanoparticles has already been established against several bacterial species: methicillin-resistant S. aureus and Bacillus subtilis; Gram-negative organisms S. cholerasuis and P. aeruginosa; and yeast species Candida albicans [31]. The bactericidal activity of Cu nanoparticles depends on the level of agglomeration, and when agglomeration has been successfully minimized, the surface area for solubilization of copper ions and interaction with bacterial membranes increases, leading to increased toxicity [4]. Metallic and ionic forms of copper produce hydroxyl radicals that damage essential proteins and DNA [32]. Similarly, CuO nanoparticles have also demonstrated antimicrobial activity against a range of Gram-positive and Gram-negative bacteria [33,34]. The CuO nanoparticles were reportedly effective in killing a range of bacterial pathogens involved in hospital-acquired infections even though higher concentrations of CuO nanoparticles were required to achieve a bactericidal effect [35]. However, the major limitation of metallic copper oxide particles in the nano-size range is lack of sufficient stability of their dispersions due to their strong tendency to aggregate and form larger clusters to reduce the energy associated with their high surface area [36]. The cluster formation is followed by rapid sedimentation leading to loss of reactivity and bactericidal applications in which a nanometric size is required [36]. Studies to determine the potential of CuO nanoparticles embedded within a polymer material have shown a lower contact-killing ability as opposed to release killing ability against methicillin-resistant S. aureus strains, thereby suggesting a release of ions into the local environment for optimal antimicrobial activity [35].

In our work of investigating antimicrobial efficacy of PSF/PVP/Cu and PSF/PVP/CuO membranes, there was a clear zone of inhibition for the membranes (Fig. 13), which represents antibacterial effect of the nanoparticles loaded PSF/PVP membranes. In particular, the diameter of bacterial inhibition zone for PSF/PVP/CuO (32.0 mm) (Fig. 13B) showed the highest inhibitory efficiency compared to the PSF/PVP/Cu (22.0 mm) (Fig. 13A) membrane. The inhibitory efficiency of the nanoparticle PSF/PVP membranes could be attributed to the presence of increased number of nanoparticles on the surface of the PSF/PVP nanofibers, with no evidence of leaching of the nanoparticles, thereby presenting PSF/PVP blend as a suitable polymer material for securing Cu and CuO nanoparticles. Furthermore, PSF/PVP/CuO supposedly had a high distribution of CuO nanoparticles on the surface, thereby leading to high bacterial inhibition. Against this background, PSF/PVP based Cu and CuO membranes have demonstrated antibacterial activities which position the membranes as attractive materials for use in water filtration, protective clothing and wound healing.

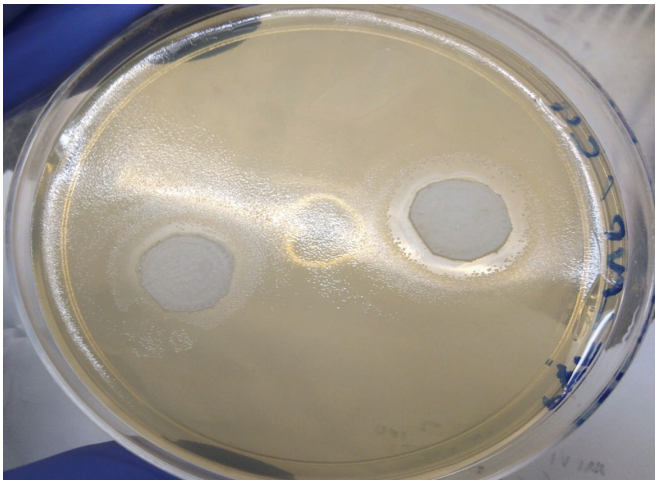

Fig. 13A Bacterial inhibition zone for PSF/PVP/Cu membrane

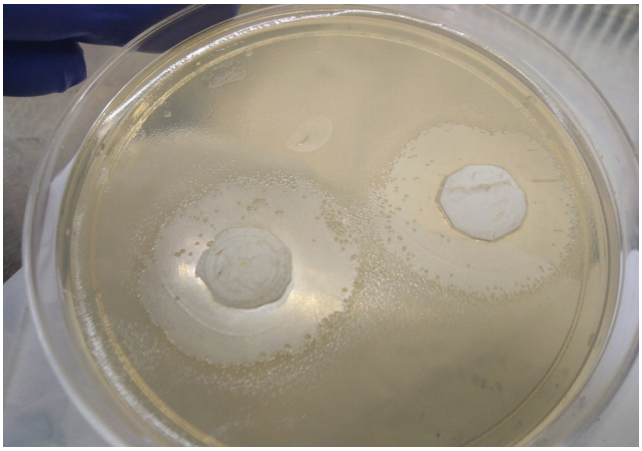

Fig. 13B Bacterial inhibition zone for PSF/PVP/CuO membrane

4. Conclusion

PSF/PVP/Cu and PSF/PVP/CuO composite membranes have been successfully prepared in this work. The membranes have been fully characterized to justify their formation. SEM images of the composite membranes clearly demonstrated the presence of nanoparticles on the fiber surfaces. The PSF/PVP based Cu and CuO nanoparticles exhibited strong antibacterial activity

against *E.coli*, thereby positioning the membranes as potential antibacterial materials for water filtration, protective clothing and wound healing. There was no leaching of nanoparticles into the aqueous media, thereby making PSF/PVP blend a suitable material for housing nanoparticles.

Acknowledgement

The authors heartily acknowledge the financial support from Botswana Institute for Technology Research and Innovation.

References

[1] V. K. Truong, N. P. Truong, and S. A. Rice, "Antibacterial Activity of Nanoparticles," *Nanomaterials*, vol. 11, no. 6, p. 1391, May 2021, doi: 10.3390/nano11061391.

[2] G. Ren, D. Hu, E. W. C. Cheng, M. A. Vargas-Reus, P. Reip, and R. P. Allaker, "Characterisation of copper oxide nanoparticles for antimicrobial applications," *International Journal of Antimicrobial Agents*, vol. 33, no. 6, pp. 587–590, Jun. 2009, doi: 10.1016/j.ijantimicag.2008.12.004.

[3] L. Wang, C. Hu, and L. Shao, "The antimicrobial activity of nanoparticles: Present situation and prospects for the future," *International Journal of Nanomedicine*, vol. 12, pp. 1227–1249, 2017, doi: 10.2147/IJN.S121956.

[4] S. S. N. Fernando, T. D. C. P. Gunasekara, and J. Holton, "Antimicrobial activity of copper-based nanoparticles against Gram-positive and Gram-negative bacteria," *Sri Lankan Journal of Infectious Diseases*, vol. 8, no. 1, pp. 2–11, 2018, doi: 10.4038/sljid.v8i1.8161.

[5] C. Zhang, R. Sun, and T. Xia, "Mechanisms of engineered nanomaterial-induced oxidative stress: A comparative study of nano- and bulk-sized particles," *Nano Today*, vol. 34, p. 100909, 2020, doi: 10.1016/j.nantod.2020.100909.

[6] S. S. N. Hona, R. Dangol, J. Ghatane, D. Giri, and R. R. Pradhananga, "Antibacterial activity of copper nanoparticles against multidrug-resistant human pathogens," *International Journal of Applied Sciences and Biotechnology*, vol. 2, no. 4, pp. 495–500, 2014, doi: 10.3126/ijasbt.v2i4.11563.

[7] H. Qamar, S. Rehman, D. K. Chauhan, A. K. Tiwari, and V. Upmanyu, "Nanoparticles: A promising approach for drug delivery and biomedical applications," *International Journal of Nanomedicine*, vol. 15, pp. 2541–2553, 2020, doi: 10.2147/IJN.S247353.

[8] D. Alagarasan, A. Harikrishnan, M. Surendiran, K. Indira, A. S. Khalifa, and B. H. Elesawy, "Green synthesis and characterization of copper nanoparticles using Ocimum sanctum leaf extract and their antimicrobial activity," *Applied Nanoscience*, 2021, doi: 10.1007/s13204-021-02054-5.

[9] M. E. Grigore, E. R. Biscu, A. M. Holban, M. C. Gestal, and A. M. Grumezescu, "Methods of synthesis, properties and biomedical applications of metallic nanoparticles," *Pharmaceuticals*, vol. 9, no. 4, p. 75, 2016, doi: 10.3390/ph9040075.

[10] S. Rezaee and M. R. Moghbeli, "Preparation and characterization of copper nanoparticles by chemical reduction method," *Iranian Journal of Chemical Engineering*, vol. 11, no. 1, pp. 45–58, 2014.

[11] K. A. G. Peroja, N. A. L. Tuberon, and K. A. Garcia, "Nanotechnology: Its applications and impact on society," *Global Scientific Journal*, vol. 7, pp. 264–311, 2019.

[12] N. I. M. Fadilah, I. L. M. Isa, W. Safwani, W. K. Zaman, Y. Tabata, and M. B. Fauzi, "The potential of collagen and hyaluronic acid in hydrogel-based scaffolds for tissue engineering applications: A review," *Polymers*, vol. 14, no. 3, p. 476, 2022, doi: 10.3390/polym14030476.

[13] L.-Y. Yu, H.-M. Shen, and Z.-L. Xu, "PVDF–TEOS hybrid hydrophobic–hydrophilic ultrafiltration membrane with antifouling property," *Journal of Applied Polymer Science*, vol. 113, no. 3, p. 1763, 2009, doi: 10.1002/app.30194.

[14] C. J. Mortimer and C. J. Wright, "The impact of nanomaterials on cell biology and medicine," *Biotechnology Journal*, 2017, doi: 10.1002/biot.201600693.

[15] S. Agarwal, J. H. Wendorff, and A. Greiner, "Use of electrospinning technique for biomedical applications," *Polymer*, vol. 49, no. 26, pp. 5603–5621, 2008, doi: 10.1016/j.polymer.2008.09.014.

[16] O. Serbanescu, S. I. Voicu, and V. K. Thakur, "Biocompatible nanocomposite membranes for biomedical applications," *Materials Today Chemistry*, vol. 17, p. 100302, 2020, doi: 10.1016/j.mtchem.2020.100302.

[17] S. Kheirieh, M. Asghari, and M. Afsari, "A review on nanocomposite membranes for water treatment," *Reviews in Chemical Engineering*, vol. 34, no. 5, pp. 657–693, 2018, doi: 10.1515/revce-2016-0065.

[18] A. Febriasari, Huriya, A. H. Ananto, M. Suhartini, and S. Kartohardjono, "Polyvinyl alcohol/sodium alginate composite membranes for pervaporation separation of ethanol–water mixtures," *Membranes*, vol. 11, no. 1, pp. 2–17, 2021, doi: 10.3390/membranes11010002.

[19] H. T. V. Nguyen, T. H. A. Ngo, K. D. Do, M. N. Nguyen, N. T. T. Dang, T. T. H. Nguyen, V. Vien, and T. A. Vu, "Synthesis and characterization of chitosan-based nanocomposite membranes for water purification," *Journal of Chemistry*, vol. 2019, pp. 1–10, 2019, doi: 10.1155/2019/1234567.

[20] M. B. Gawande, A. Goswami, F.-X. Felpin, T. Asefa, X. Huang, R. Silva, X. Zou, R. Zboril, and R. S. Varma, "Cu and Cu-based nanoparticles: Synthesis and applications in catalysis," *Chemical Reviews*, vol. 116, no. 6, pp. 3722–3811, 2016, doi: 10.1021/acs.chemrev.5b00482.

[21] Z. Zhou, C. Lu, X. Wu, and X. Zhang, "Cellulose nanocrystals as a reinforcing material for electrospun poly(vinyl alcohol) nanofibers," *RSC Advances*, vol. 3, no. 42, pp. 26066–26073, 2013, doi: 10.1039/c3ra43891h.

[22] M. Balouiri, M. Sadiki, and S. K. Ibnsouda, "Methods for in vitro evaluating antimicrobial activity: A review," *Journal of Pharmaceutical Analysis*, vol. 6, no. 2, pp. 71–79, 2016, doi: 10.1016/j.jpha.2015.11.005.

[23] A. Maoa, M. Ding, X. Jin, X. Gu, C. Cai, C. Xin, and T. Zhang, "Synthesis, characterization and antibacterial activity of copper nanoparticles," *Journal of Molecular Structure*, vol. 1079, pp. 396–401, 2015, doi: 10.1016/j.molstruc.2014.09.049.

[24] D. Devipriya and S. M. Roopan, "Biogenic nano-catalyst: An eco-friendly approach for the synthesis of nanoparticles," *Materials Science and Engineering*: C, vol. 80, pp. 38–44, 2017, doi: 10.1016/j.msec.2017.05.004.

[25] A. Sarkar, T. Mukherjee, and S. Kapoor, "Synthesis and

catalytic application of copper nanoparticles supported on alumina," *Journal of Physical Chemistry C*, vol. 112, no. 9, pp. 3334–3340, 2008, doi: 10.1021/jp0773767.

[26] A. Eslami, N. M. Juibari, S. G. Hosseini, and M. Abbasi, "Preparation and characterization of energetic nanocomposites based on nitrocellulose and nano-Al," *Central European Journal of Energetic Materials*, vol. 14, no. 1, pp. 152–168, 2017, doi: 10.22211/cejem/69352.

[27] N. Savage and M. S. Diallo, "Nanomaterials and water purification: Opportunities and challenges," *Journal of Nanoparticle Research*, vol. 7, no. 4–5, p. 331, 2005, doi: 10.1007/s11051-005-4877-0.

[28] K. De Prijck, H. Nelis, and T. Coenye, "In vitro assessment of the activity of antimicrobial agents against bacterial biofilms by means of the MBEC assay," *Biofouling: Journal of Bioadhesion and Biofilm Research*, vol. 23, no. 5, p. 405, 2007, doi: 10.1080/08927010701316432.

[29] H. Khalid, S. Shamaila, and N. Zafar, "Green synthesis of copper nanoparticles using plant extracts and their antimicrobial activity," *Materials Science International*, vol. 27, pp. 3085–3088, 2015, doi: 10.1016/j.msint.2015.07.012.

[30] K. K. Dey, P. Kumar, R. R. Yadav, A. Dhar, and A. K. Srivastava, "Facile synthesis of copper nanoparticles and their catalytic application in reduction of nitroaromatics," *RSC Advances*, vol. 4, no. 1, p. 101, 2014, doi: 10.1039/c3ra45912a.

[31] L. Wang, C. Hu, and L. Shao, "The antimicrobial activity of nanoparticles: Present situation and prospects for the future," *International Journal of Nanomedicine*, vol. 12, pp. 1227–1249, 2017, doi: 10.2147/IJN.S121956.

[32] A. Chatterjee and R. Chakra, "Nanoparticle-based approaches in nanotechnology: A review," *Nanotechnology*, vol. 25, no. 1, pp. 1–23, 2014, doi: 10.1088/0957-4484/25/1/012001.

[33] M. Ahamed, H. A. Alhadlaq, M. A. M. Khan, P. Karuppiah, and N. A. Al-Dhabi, "Synthesis, characterization, and antimicrobial activity of copper oxide nanoparticles," *Journal of Nanomaterials*, vol. 2014, Article ID 637858, 4 pages, 2014, doi: 10.1155/2014/637858.

[34] F. A. Bezza, S. M. Tichapondwa, and E. M. N. Chirwa, "Microbial mediated synthesis of iron oxide nanoparticles for water treatment," *Scientific Reports*, vol. 10, Article ID 16680, 2020, doi: 10.1038/s41598-020-73709-4.

[35] G. Ren, D. Hu, E. W. C. Cheng, M. A. Vargas-Reus, P. Reip, and R. P. Allaker, "Characterization of copper oxide nanoparticles for antimicrobial applications," *International Journal of Antimicrobial Agents*, vol. 33, no. 6, pp. 587–590, 2009, doi: 10.1016/j.ijantimicag.2008.12.004.

[36] E. M. Hotze, T. Phenrat, and G. V. Lowry, "Nanoparticle transport, fate, and toxicity in the environment: Current knowledge and future directions," *Journal of Environmental Quality*, vol. 39, no. 6, pp. 1909–1924, 2010, doi: 10.2134/jeq2009.0427.